STEM CELLS AND DEVELOPMENT
Volume 23, Number 9, 2014

DOI: 10.1089/scd.2013.0486

Dimethyloxaloylglycine Increases the Bone Healing Capacity of Adipose-Derived Stem Cells by Promoting Osteogenic Differentiation and Angiogenic Potential

Hao Ding,[1,*] You-Shui Gao,[1,*] Yang Wang,[1] Chen Hu,[2] Yuan Sun,[1] and Changqing Zhang[1]

Hypoxia inducible factor-1α (*HIF-1α*) plays an important role in angiogenesis-osteogenesis coupling during bone regeneration, which can enhance the bone healing capacity of mesenchymal stem cells (MSCs) by improving their osteogenic and angiogenic activities. Previous studies transduced the *HIF-1α* gene into MSCs with lentivirus vectors to improve their bone healing capacity. However, the risks due to lentivirus vectors, such as tumorigenesis, should be considered before clinical application. Dimethyloxaloylglycine (DMOG) is a cell-permeable prolyl-4-hydroxylase inhibitor, which can activate the expression of *HIF-1α* in cells at normal oxygen tension. Therefore, DMOG is expected to be an alternative strategy for enhancing *HIF-1α* expression in cells. In this study, we explored the osteogenic and angiogenic activities of adipose-derived stem cells (ASCs) treated with different concentrations of DMOG in vitro, and the bone healing capacity of DMOG-treated ASCs combined with hydrogels for treating critical-sized calvarial defects in rats. The results showed that DMOG had no obvious cytotoxic effects on ASCs and could inhibit the death of ASCs induced by serum deprivation. DMOG markedly increased vascular endothelial growth factor production in ASCs in a dose-dependent manner and improved the osteogenic differentiation potential of ASCs by activating the expression of *HIF-1α*. Rats with critical-sized calvarial defects treated with hydrogels containing DMOG-treated ASCs had more bone regeneration and new vessel formation than the other groups. Therefore, we believe that DMOG enhanced the angiogenic and osteogenic activity of ASCs by activating the expression of *HIF-1α*, thereby improving the bone healing capacity of ASCs in rat critical-sized calvarial defects.

Introduction

The treatment of large bone defects caused by severe trauma, resection of tumors, and congenital deformities is still a challenge in orthopedic surgery and requires the application of various bone substitutes. However, limited success has been achieved in treating large bone defects with bone substitutes alone, such as tricalcium phosphate, hydroxyapatite, or coralline scaffolds [1]. Bony ingrowth and vascularization are often limited to the periphery of the scaffolds as they lack adequate capability to induce osteogenesis and angiogenesis. Therefore, tissue engineering studies have explored the use of various cells and biological factors in combination with these scaffolds to improve their osteogenic and angiogenic activities [2,3].

In previous studies, mesenchymal stem cells (MSCs) were widely used with bone substitutes to promote new bone repair and regeneration [4,5]. These cells have osteogenic differentiation potential and can differentiate into osteoblasts to promote osteogenesis [6,7]. They also secrete many angiogenic growth factors, which promote local revascularization. Angiogenesis is a fundamental step in new bone formation, and neovascularization promotes bone regeneration [8,9]. However, large numbers of seed cells are needed for the successful repair of a large defect. Due to this requirement, treated cells that have enhanced osteogenic and angiogenic capacity are beneficial in the application of cells for bone regeneration in tissue engineering studies.

Hypoxia inducible factor-1α (*HIF-1α*) is a crucial mediator of the adaptive cell response to hypoxia, and plays an important role in angiogenesis-osteogenesis coupling during bone regeneration [10]. It controls the activity of a broad array of genes and modulates cell proliferation, differentiation, and pluripotency [11]. *HIF-1α* can promote the secretion of vascular endothelial growth factor (*VEGF*) in MSCs, is a potent mitogen for endothelial cells (ECs), and plays a central role in neovascularization and angiogenesis [12]. Angiogenesis helps support MSCs and osteoblasts that

[1]Department of Orthopedic Surgery, Shanghai Sixth People's Hospital, Shanghai Jiao Tong University, Shanghai, China.
[2]Shanghai Key Laboratory of Regulatory Biology, School of Life Sciences, East China Normal University, Shanghai, China.
*These authors contributed equally to this work.

are necessary for bone repair, and is coupled with osteogenesis in bone repair and regeneration [13–15]. *VEGF* also has direct effects on osteoblast lifespan and function, and regulates the communication between osteoblasts and ECs [16–18]. It was also reported that *HIF-1α* improves the osteogenic differentiation capacity of MSCs and enhances their osteogenic activity [19]. Therefore, overexpression of *HIF-1α* in MSCs enhances their osteogenic and angiogenic activities and promotes the repair of large bone defects.

Previous studies transduced the *HIF-1α* gene into MSCs with lentivirus vectors, and found that *HIF-1α* transgenic MSCs had better osteogenic and angiogenic capacity in vitro and in vivo, leading to better bone healing potential in large bone defects [20–22]. However, once transduced into cells, the *HIF-1α* gene will, theoretically, be overexpressed throughout the cell's life. In addition, the risks of lentivirus vectors, such as tumorigenesis, should be seriously considered before clinical application. Dimethyloxaloylglycine (DMOG) is a small molecular drug, and is a cell-permeable prolyl-4-hydroxylase inhibitor. At normal oxygen tension, hypoxia-inducible factor prolyl hydroxylase (HIF-PH) hydroxylates a specific proline residue of *HIF-1α*, which promotes *HIF-1α* binding to the Von Hippel-Lindau tumor suppressor, and causes the degradation of *HIF-1α*. DMOG can inhibit the effect of HIF-PH, and thus stabilize the expression of *HIF-1α* in cells [23]. Therefore, DMOG is expected to be an alternative strategy for enhancing *HIF-1α* expression in cells, which may be safely used in the clinic.

In previous studies, by activating the expression of *HIF-1α*, DMOG has been successfully used to attenuate post-ischemic myocardial injury [24] and renal injury in remnant kidney [25], induce angiogenesis in ischemic skeletal muscles [26], and provide neuroprotection in a middle cerebral artery occlusion model [27]. However, to our knowledge, there are no reports on the effects of DMOG on the bone healing capacity of MSCs. Adipose-derived stem cells (ASCs) are an important type of MSCs, which are easy to harvest with liposuction and are abundant, leading to minimal donor site morbidity and a reduced period of in vitro expansion. In this study, we explored the influence of DMOG on the osteogenic and angiogenic potential of ASCs, and its bone healing capacity in the treatment of critical-sized calvarial defects in rats.

Materials and Methods

Cell harvest and culture

All procedures adhered to the recommendations of the U.S. Department of Health for the care and use of laboratory animals and were approved by the Ethics Committee of Shanghai Jiao Tong University. Primary ASCs were harvested from the adipose tissue of F344 rats (Shanghai Animal Experimental Center, Shanghai, China) as previously reported [28]. Briefly, adipose tissues were harvested from the animals under anesthesia (pentobarbital sodium; Sigma, St. Louis, MO) and then digested with 0.1% collagenase I (Sigma) for 60 min at 37°C. The tissue was filtered through a 100-μm nylon mesh (Shanghai Bolting Cloth Manufacturing Co., Ltd, Shanghai, China), and the filtrate was centrifuged at 1,500 rpm (363*g*). The cells were then plated on culture dishes (Corning, Tewksbury, MA) and cultured in Dulbecco's modified Eagle's medium (DMEM; Gibco BRL, Grand Island, NY) supplemented with 10% fetal bovine serum (FBS; Invitrogen, Carlsbad, CA) at 37°C in a humidified 5% CO_2 incubator. The culture medium was replaced every 3 days and cells were passaged when they reached ~80% confluence with 0.25% trypsin (Invitrogen). Flow cytometry (BD Biosciences, San Jose, CA) was used to characterize ASCs with CD29, CD31, CD34, CD44, CD45, and CD90 (BD Biosciences). To avoid contamination by hematopoietic cells in earlier passages and differentiated cells in later passages, cells of four to six passages were used for the following experiments.

Cell proliferation and survival evaluation

To determine the influence of DMOG on ASCs proliferation, cells were seeded on plates and then treated with different concentrations of DMOG (Sigma; 0, 200, 500, and 1,000 μM) for 24, 48, and 72 h. Cell numbers were measured using the Cell Counting Kit-8 (CCK-8; Beyotime Institute of Biotechnology, Shanghai, China) and a Microplate Reader (450 nm; Bio-Rad, Hercules, CA). Trypan blue staining was performed to assess the cell death ratio, a possible indication of the toxicity of DMOG. Briefly, trypan blue (Invitrogen) was added to the medium at a final concentration of 0.05%. After 10 min of incubation, images of six different randomly chosen fields per well were taken under the microscope. Cell death was calculated by the ratio of trypan-blue-positive cells to total cells. The influence of DMOG on cell survival in serum deprivation conditions was also evaluated using trypan blue staining. ASCs were plated in six-well plates (Corning) and cultured in regular medium for 12 h. The cells were then washed with phosphate-buffered saline (PBS) and cultured in serum-free medium with different concentrations of DMOG. After 24, 48, and 72 h, trypan blue staining was performed.

HIF-1α shRNA construction and transfection

To inhibit the expression of *HIF-1α* in ASCs, the *HIF-1α* shRNA (forward oligo: 5′ T CCAGTTGAATCTTCAGATA TTCAAGAGA TATCTGAAGATTCAACTGG TTTTTT C 3′, reverse oligo: 5′ TCGAGAAAAAA CCAGTTGAATCT TCAGATA TCTCTTGAA TATCTGAAGATTCAACTGG A 3′; Invitrogen) was constructed by the pll3.7(Lentilox 3.7)-Zsgreen vector (Addgene, Cambridge, MA). For infection, ASCs were plated on a 12-well plate (Corning) at 5×10^4 cells and infected with shRNA lentivirus at an MOI of 100 in the presence of 8 μg/mL polybrene (Sigma). To determine the infection efficiency of the lentivirus, shHIF-1α ASCs were reflected by the GFP-positive proportion of cells detected by flow cytometry, and the results showed that more than 85% were GFP positive 48 h after infection.

Western blot analysis

To evaluate the influence of DMOG on the expression of *HIF-1α* and *VEGF* in ASCs, the cells were cultured in regular medium with DMOG (0, 200, 500, and 1,000 μM) under normal oxygen conditions. After 24 h, total protein was harvested from the cultured cells according to standard protocols. The protein concentration of the cells was measured with a BCA protein assay kit (Thermo, Rockford, IL).

The cell lysates were then separated on SDS-PAGE (Bio-Rad) using 12% gels (Bio-Rad) and transferred to nitrocellulose membranes (Whatman). The membranes were incubated with primary antibodies of *HIF-1α* (Abcam, Cambridge, MA) and *VEGF* (Abcam) at a 1:800 dilution overnight, followed by incubation with infrared-conjugated secondary antibodies (Odyssey) at 1:10,000 for 1 h at room temperature. The membranes were scanned in an Odyssey Scanner (Li-COR Biosciences, Lincoln, NE), and bands were quantified using Odyssey software V3.0. The protein levels were normalized against *β-actin*. shHIF-1α ASCs cultured in regular medium with 1,000 μM DMOG were used as controls.

Enzyme-linked immunosorbent assay for VEGF

To analyze *VEGF* production by ASCs treated with DMOG, ASCs were cultured in regular medium with different concentrations of DMOG (0, 200, 500, and 1,000 μM). shHIF-1α ASCs exposed to 1,000 μM DMOG were also included in the study. After 1, 3, 7, 14, and 21 days, the cells were seeded into six-well plates at 300,000 cells per well. After incubation in regular medium with different concentrations of DMOG for 24 h, the medium was harvested and stored at −80°C until analysis of the *VEGF* protein using an enzyme-linked immunosorbent assay (ELISA) kit (Antibodies-Online, Aachen, Germany) according to the manufacturer's instructions. The total protein content of these cells was then determined for standardization of *VEGF* production with a BCA protein assay kit (Pierce Biotechnology, Rockford, IL).

Quantitative real-time polymerase chain reaction analysis

To verify whether DMOG improved the osteogenic differentiation potential of ASCs, cells (1×10^5) were plated on six-well plates and cultured in osteogenic differentiation medium (No. A10072-01; Gibco BRL) with different concentrations of DMOG (0, 200, 500, and 1,000 μM). shHIF-1α ASCs exposed to 1,000 μM DMOG were also included in this study. Total cellular RNA was harvested with TRIzol (Invitrogen) at days 1, 3, 7, 14, and 21 after osteogenic induction, according to the manufacturer's protocol. One microgram of purified RNA was then reverse transcribed using the PrimeScript RT reagent kit (Takara, Shiga, Japan) according to the manufacturer's protocol. The reverse transcription reaction was mixed with iQ SYBR Green super mix and amplified with the iQ5 real-time system. The product was quantified using a standard curve, and all values were normalized to glyceraldehyde-3-phosphate dehydrogenase (*GAPDH*). Primers were designed with the assistance of PrimerBank and are listed in Table 1.

Alkaline phosphatase activity and alizarin red-S staining

The in vitro osteogenic capacity of ASCs exposed to DMOG was then confirmed by determining the deposition of mineralized matrix with alizarin red-S (ARS) staining 21 days after osteogenic induction. Cell cultures were fixed in neutral-buffered formalin (Sinopharm Chemical Reagent Co., Ltd, Shanghai, China) for 30 min and stained with ARS (Sigma) for 30 min. The cultures were then evaluated by light microscopy and calcium deposition was confirmed by the formation of red nodules. Quantification was performed using a colorimetric assay. The cultures were incubated with 20% methanol/10% acetic acid solution (Sinopharm Chemical Reagent Co., Ltd) for 15 min followed by optical density determination at 450 nm. The alkaline phosphatase (*ALP*) activity was also determined in cell lysates using an *ALP* kit (Catalog No. GTX85593; Gene Tex, Irvine, CA) 14 days after osteogenic induction, according to the manufacturer's instructions. Values were measured at 420 nm optical density and normalized against the protein concentration measured with a BCA protein assay kit (Pierce Biotechnology).

Preparation of transplanted composite

BeaverNano™ hydrogel (Cyagen, Guangzhou, China), a self-assembling peptide gel, was used as the scaffold to load the cells. By mixing with fluids containing polyvalent metal ions, the hydrogels can form three-dimensional (3D) nanofiber networks, which can support cell migration, proliferation, and differentiation within the network. The hydrogels were mixed with cells according to the manufacturer's protocol. Briefly, cells were suspended in 10% sucrose solution (Sinopharm Chemical Reagent Co., Ltd) at 4×10^6 cells/mL and evenly mixed with the hydrogels in an equal volume. PBS (Sinopharm Chemical Reagent Co., Ltd) was then added to the mixed hydrogel composites at 1:1 and incubated for 30 min to allow cross-linking. The cell/hydrogel composites were then applied to the critical-sized calvarial bone defects in rats. For groups implanted with normal or shHIF-1α ASCs treated with DMOG, cells were cultured in medium with 1,000 μM DMOG for 24 h before mixing with the hydrogel. To ensure the cells were exposed to DMOG in vivo, DMOG was added to PBS during the hydrogel mixing procedure and the mixed hydrogel composites in the two groups contained 1,000 μM DMOG.

Animal surgery and protocol

To evaluate the in vivo bone healing capacity of DMOG-treated ASCs, critical-sized calvarial defects in the parietal bones of rats were performed. The rats were randomly divided into four groups. Group I ($n = 12$) underwent implantation of hydrogels alone. Group II ($n = 12$) underwent implantation of hydrogels mixed with normal ASCs. Group III ($n = 12$) underwent implantation of hydrogels mixed with shHIF-1α ASCs treated with 1,000 μM DMOG. Group IV ($n = 12$) underwent implantation of hydrogels mixed with normal ASCs treated with 1,000 μM DMOG. Following anesthesia with intraperitoneal pentobarbital (3 mg/100 g; Sigma), two 5-mm defects in the frontal parietal bone were carefully made using a trephine drill (Nouvag AG, Goldach, Switzerland), avoiding damage to the dura mater. The hydrogels with or without cells were then implanted into the defects in the parietal bones. Eight weeks after surgery, rats were euthanized and perfused with Microfil (Microfil MV-122; Flow Tech, Carver, MA). In brief, the animals were anesthetized and the rib cage was opened. The descending aorta was clamped and the inferior vena cava was incised.

Table 1. Quantitative Real-Time Polymerase Chain Reaction Primer Sequences

Gene	*Forward primer*	*Reverse primer*
Runx-2	CCTCACAAACAACCACAGAACCA	AACTGAAAATACAAACCATACCC
OCN	AAGCAGGAGGGCAGTAAGGT	AGCAGCTGTGCCGTCCATAC
ALP	ATTTTTGGTCTGGCTCCCATG	TCTCCCGTTCACCGTCCAC
GAPDH	TGACCACAGTCCATGCCATCAC	CGCCTGCTTCACCACCTTCTT

Then, heparinized saline (Shanghai No.1 Biochemical & Pharmaceutical Co., Ltd, Shanghai, China) and Microfil were successively perfused into the left ventricle with an angiocatheter. Subsequently, the rats were stored at 4°C for 1 h to ensure polymerization of the contrast agent.

Evaluation of osteogenesis in vivo

The evaluation of osteogenesis in vivo was performed at 8 weeks after surgery. After harvesting the parietal bone, micro-CT scanning was performed to evaluate new bone formation in the calvarial defect area. The scan was performed using a high-resolution micro-CT II scanner (SkyScan 1076, Kontich, Belgium) at the following settings: X-ray voltage of 80 KVp, anode current of 450 μA, and an exposure time of 400 ms. The images were segmented with a low-pass filter to remove noise, and a threshold of 800 was defined as bone tissue. The parameters of new bone volume (BV)/total volume (TV) and bone mineral density (BMD) of the bone defect area were then calculated.

After micro-CT scanning, six samples from each group were dehydrated in alcohol from 70% to 100%, and embedded in polymethylmethacrylate (PMMA; Sinopharm Chemical Reagent Co., Ltd). The sagittal sections, which represented the central area of the defect, were cut with a microtome (Leica, Germany) and polished to a final thickness of ~40 mm, as previously reported [29]. The sections were then stained with van Gieson's picrofuchsin according to standard procedures. To evaluate new bone formation, the surface areas of the newly formed bone were measured based on the entire defect area using a Leica digital imaging system and NIH image analysis software. Averages for each sample and each group were then calculated.

Evaluation of angiogenesis in vivo

After micro-CT scanning of bone regeneration, six samples from each group were fixed in 4% paraformaldehyde (Sinopharm Chemical Reagent Co., Ltd) and decalcified with 10% ethylene diamine tetra acetic acid (EDTA; Sinopharm Chemical Reagent Co., Ltd) for 3 days. Then, micro-CT was performed again to evaluate new vessel formation at a resolution of 18 μm per voxel. For segmentation of blood vessels from background, noise was removed by a low-pass Gaussian filter. The blood vessels were then included with semiautomatically drawn contours at each two-dimensional section by the built-in ''Contouring Program'' (SkyScan CTAn software) for automatic reconstruction of 3D images of vasculature. The number of vessels in the bone defect area was then counted, and the total vessel volume represented by all voxels in the specified Microfil range was calculated.

Immunohistochemistry

After micro-CT, the decalcified samples were embedded in paraffin and sectioned at 5 μm at the central area of the defect. Immunohistochemistry for *HIF-1α* (ab8366, 1:100; Abcam), osteocalcin (*OCN*, ab13420, 1:100; Abcam), and CD31 (ab24590, 1:200; Abcam) was then performed in the sections from each group. Briefly, the sections were rehydrated, treated with antigen retrieval, and incubated with the primary antibody at 4°C overnight. Subsequently, the biotinylated secondary antibody and ABC complex were applied and DAB substrate was used to stain the sections. The sections were then treated with hematoxylin and mounted. The results were analyzed with a light microscope.

Statistical analysis

All of the in vitro experiments were performed in triplicate and data were presented as mean ± SD. Statistical analysis of the data was performed using ANOVA with an SNK post hoc analysis. P values < 0.05 were considered statistically significant.

Results

DMOG suppresses ASC proliferation and enhances ASC survival

The ASCs showed the potential of osteogenic (Fig. 1A), adipogenic (Fig. 1B), and chondrogenic differentiation (Fig. 1C). It also had high expression of MSC markers CD29, CD44, and CD90, whereas low expression of the hematopoietic lineage markers CD31, CD34, and CD45 (Fig. 1D). To determine the influence of DMOG on ASCs proliferation, the numbers of ASCs treated with different concentrations of DMOG were measured with the CCK-8. ASCs proliferation was significantly suppressed after 48 and 72 h of incubation with DMOG, and this inhibition was dose dependent (Fig. 2A). ASCs death was detected using trypan blue staining after exposure to different concentrations of DMOG. There were no significant differences between the death ratio of cells with/without exposure to DMOG (Fig. 2B), which indicated that DMOG at these concentrations had no obvious toxicity in ASCs. The effects of DMOG on serum-deprivation-induced cell death were also determined. DMOG showed a dose-dependent reduction in cell death in serum deprivation conditions (Fig. 2C), which indicated that DMOG enhanced cell survival during cell stress.

DMOG promotes expression of VEGF

After treatment with different concentrations of DMOG, the expression of *HIF-1α* and *VEGF* in ASCs was detected by western blotting (Fig. 3A). The level of *HIF-1α* protein

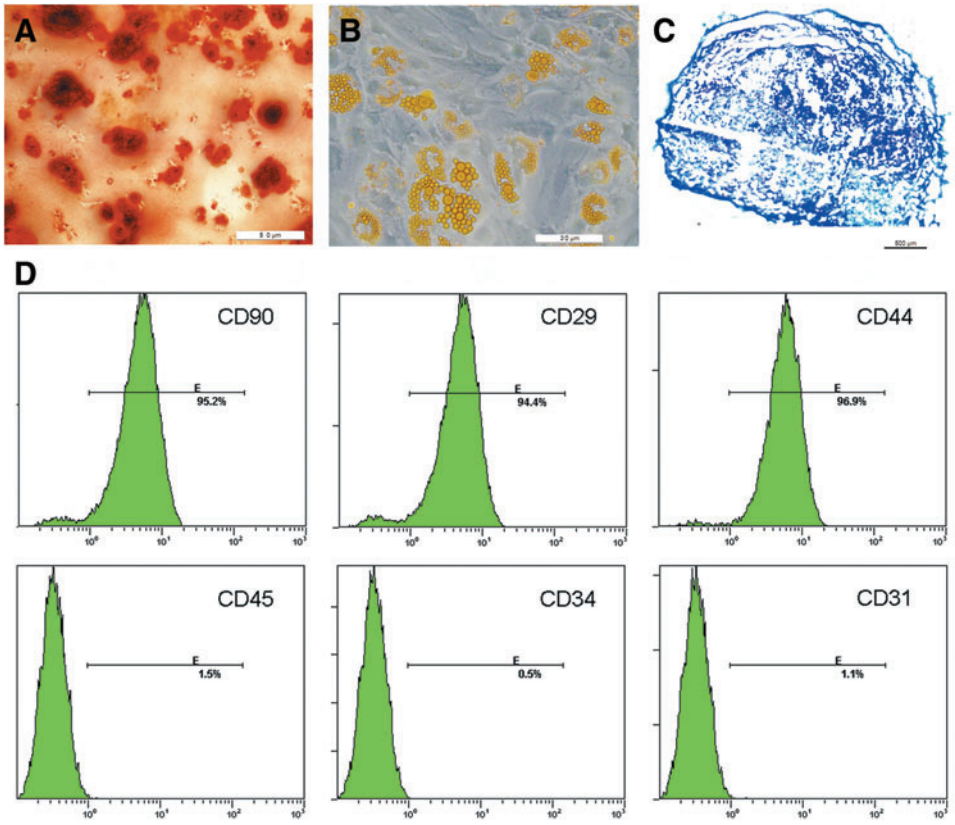

FIG. 1. The adipose-derived stem cell (ASC) potential of osteogenic, adipogenic, and chondrogenic differentiation was separately confirmed by alizarin red-S (ARS) staining **(A)**, Oil Red O staining **(B)**, and Alcian blue staining **(C)**. Flow cytometry showed that ASCs had high expression of mesenchymal stem cell markers CD29, CD44, and CD90, whereas low expression of the hematopoietic lineage markers CD31, CD34, and CD45 **(D)**. Color images available online at www.liebertpub.com/scd

was enhanced in response to DMOG treatment in a dose-dependent manner. After treatment with DMOG for 24 h, the expression of *HIF-1α* in ASCs increased to stable levels, which were ~2-, 4-, and 6-fold for 200, 500, and 1,000 μM DMOG, respectively. However, there was no notable increase in shHIF-1α ASCs treated with 1,000 μM DMOG (Fig. 3B). The level of *VEGF* protein was also enhanced after DMOG treatment in a dose-dependent manner. After treatment with DMOG for 72 h, the expression of *VEGF* in normal ASCs increased by ~4-, 7-, and 9-fold for 200, 500, and 1,000 μM DMOG, respectively. There was also no significant increase in *VEGF* expression in shHIF-1α ASCs, which indicated that the increase in *VEGF* was due to the overexpression of *HIF-1α* stabilized by DMOG (Fig. 3C).

The levels of *VEGF* secreted from cells into the culture medium were measured by ELISA (Fig. 3D). *VEGF* production in normal ASCs was very little and did not change significantly. *VEGF* production in ASCs treated with DMOG markedly increased from day 1 to 3 and was then maintained at a higher level until day 21. The increase in *VEGF* production was also dose dependent, and *VEGF* production in shHIF-1α ASCs was maintained at a lower level.

DMOG improves the osteogenic differentiation potential of ASCs

To verify whether DMOG improves the osteogenic differentiation potential of ASCs, the expression of related

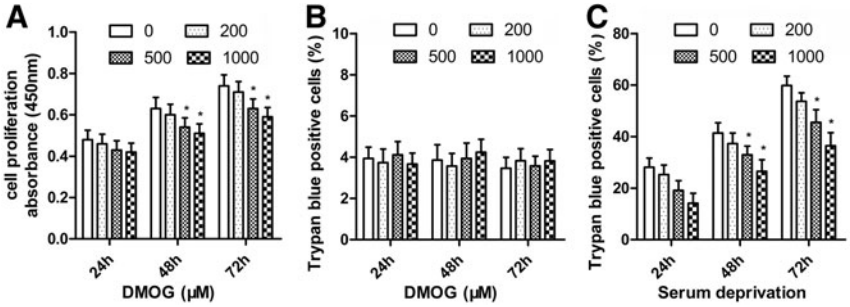

FIG. 2. Effect of dimethyloxalylglycine (DMOG) on the proliferation and survival of ASCs. **(A)** After treatment with different concentrations of DMOG, ASC proliferation was measured with the Cell Counting Kit-8 (CCK-8) and the results are expressed as the mean of absorbance ± SEM. **(B)** ASC death ratio was determined using trypan blue staining after exposure to different concentrations of DMOG. **(C)** DMOG dose-dependently reduced cell death ratio in serum deprivation conditions (*, significant difference compared with cells treated with culture medium alone, $P < 0.05$).

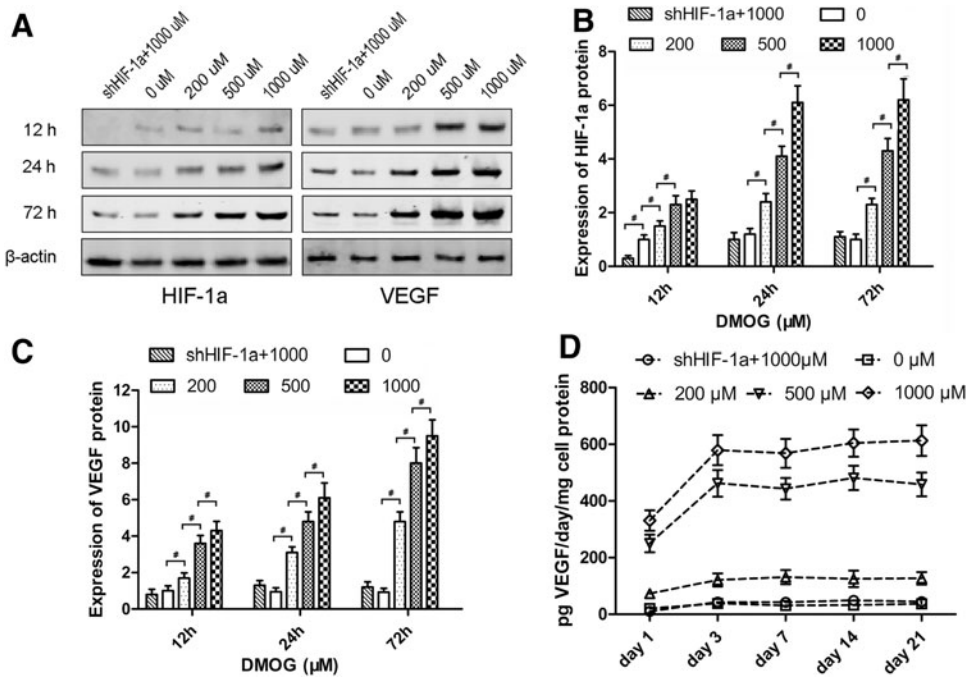

FIG. 3. Effect of DMOG on the expression of hypoxia inducible factor-1α (*HIF-1α*) and vascular endothelial growth factor (*VEGF*) in ASCs. **(A)** Western blotting showed that DMOG significantly affected the protein levels of *HIF-1α* and *VEGF* in ASCs. **(B, C)** The analysis suggested that the expression of *HIF-1α* and *VEGF* in ASCs was increased by DMOG in a dose-dependent manner, and there was no notable increase in shHIF-1α ASCs treated with 1,000 μM DMOG. **(D)** Enzyme-linked immunosorbent assay (ELISA) showed the production of *VEGF* secreted from ASCs treated with different concentrations of DMOG (#, significant difference between the two groups, $P < 0.05$).

osteogenic genes in ASCs, treated with different concentrations of DMOG, was determined by quantitative real-time polymerase chain reaction (qRT-PCR) (Fig. 4A). The transcript level for *Runx-2*, an early stage osteogenic marker, was upregulated from day 3 to 14 in normal ASCs, and the increase was significantly higher in ASCs treated with DMOG than in normal ASCs ($P < 0.05$). The expression of *OCN* and *ALP*, mature-stage bone markers, showed continued upregulation from day 7 to 21, and the increase in ASCs treated with DMOG was also higher than that in normal ASCs during this period ($P < 0.05$). However, the expression of these three osteogenic genes was not significantly enhanced in shHIF-1α ASCs treated with 1,000 μM DMOG, compared with that in normal ASCs.

ARS staining showed more calcium deposits in ASCs exposed to DMOG than in normal ASCs (Fig. 4B). Spectromorphometric quantification showed that the amount of calcium deposits increased by ~0.5-, 1.1-, and 1.4-fold after exposure to 200, 500, and 1,000 μM DMOG, respectively ($P < 0.05$; Fig. 4C). The results of the *ALP* activity assay (Fig. 4D) showed that *ALP* activity in ASCs was significantly increased after exposure to DMOG ($P < 0.05$). *ALP* activity in ASCs treated with 1,000 μM DMOG was ~2.5-fold higher than that in normal ASCs. There was no significant difference between *ALP* activity in normal ASCs and shHIF-1α ASCs treated with 1,000 μM DMOG ($P > 0.05$).

DMOG improves the bone healing capacity of ASCs in vivo

The morphology of the newly formed bone in the defect area of the parietal bone was determined with micro-CT scanning 8 weeks after surgery. In the group implanted with ASCs exposed to 1,000 μM DMOG, plate-like bone structure was formed and occupied a large part of the bone defect area observed on the coronal and sagittal surfaces (Fig. 5A). Quantitative analysis of the newly formed bone was performed using morphometric methods. There was almost no healing of the defect area in the group treated with hydrogel alone. About 23.3% of the defect area was regenerated in the group treated with normal ASCs, and the healing area was about 51.3% of the entire defect area in the group treated with ASCs exposed to 1,000 μM DMOG, which was significantly higher than that in the previously mentioned two groups. The healing area of the group treated with shHIF-1α ASCs exposed to 1,000 μM DMOG was only about 32.3% (Fig. 5B), which indicated that DMOG may improve the bone healing capacity of ASCs by enhancing the expression of *HIF-1α*. The BMD of the new bone in the four groups was also analyzed. The results demonstrated the same trends, in that BMD was highest in the group treated with ASCs exposed to 1,000 μM DMOG than in the other groups, and decreased significantly when HIF-1α expression in ASCs was inhibited by shRNA (Fig. 5C). Histological findings also showed that the undecalcified specimens in the group treated with ASCs exposed to 1,000 μM DMOG had a larger area of new bone formation in the defect than the other groups, which further supported the micro-CT data (Fig. 6).

DMOG promotes revascularization in vivo

The effects of the implanted cells on vascularization of the defect area 8 weeks after implantation were determined by perfusing the vessels with Microfil and imaging with micro-CT. The reconstructed 3D micro-CT images directly showed newly formed blood vessels in the defect area. The vessels in the defect area of the group treated with ASCs exposed to DMOG were significantly denser than those in the other three groups (Fig. 7A). Quantification of the newly formed blood vessels was performed by morphometric analysis. The number and total volume of blood vessels in the group treated with ASCs exposed to DMOG were more than those in the groups treated with normal ASCs. However, the number and total volume of blood vessels in the group treated with shHIF-1α ASCs were less than those in

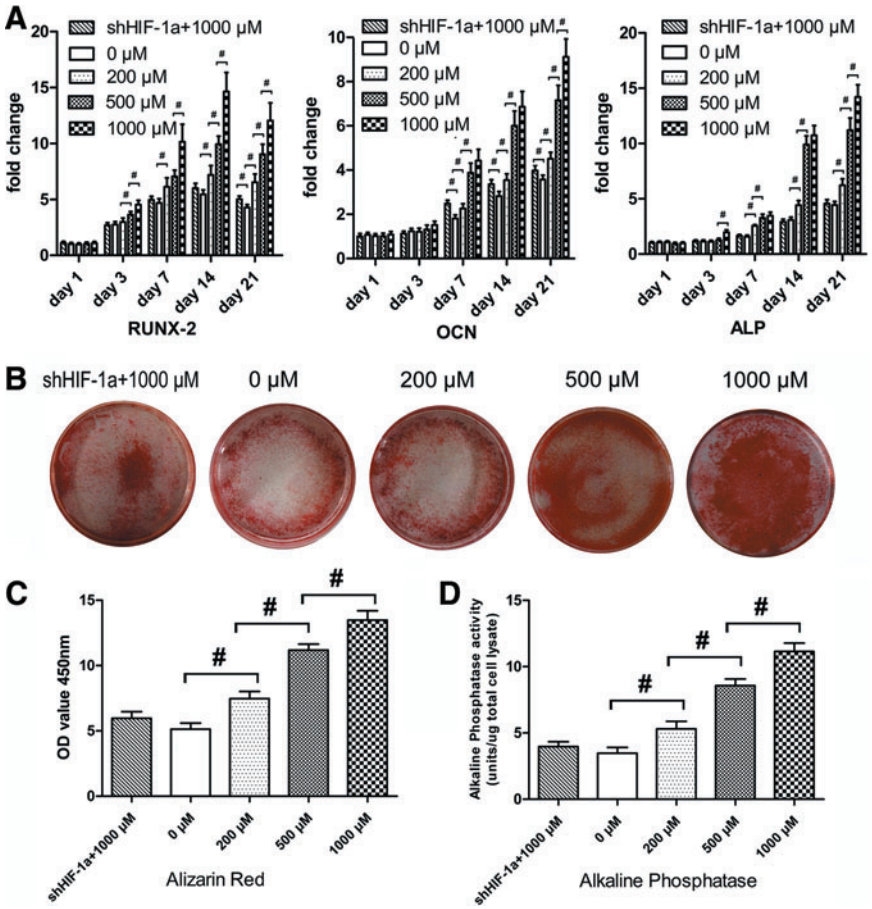

FIG. 4. Effect of DMOG on the osteogenic differentiation potential of ASCs. **(A)** ASCs and shHIF-1α ASCs were cultured in osteogenic differentiation medium with different concentrations of DMOG, and the mRNA expression levels of *RUNX-2*, osteocalcin (*OCN*), and alkaline phosphatase (*ALP*) were detected using quantitative real-time polymerase chain reaction (qRT-PCR). **(B)** ARS staining of ASCs and shHIF-1α ASCs exposed to different concentrations of DMOG. **(C)** Spectromorphometric quantification of ARS staining showed that the amount of calcium deposits was significantly increased by DMOG treatment. **(D)** Semiquantitative analysis of *ALP* activity (#, significant difference between the two groups, $P < 0.05$). Color images available online at www.liebertpub.com/scd

the group treated with ASCs exposed to DMOG, but more than those in the group treated with normal ASCs (Fig. 7B, C). This may be due to DMOG contained in the hydrogels in Group III that affected autologous bone-marrow-derived mesenchymal stem cell (BMSC) and EC migration to the defect areas, which promoted local revascularization.

Immunohistochemistry analysis

To detect *HIF-1α* expression in DMOG-treated ASCs implanted in the bone defect area, immunohistochemistry for *HIF-1α* was performed. In Groups I, II, and III, there were no obvious positive staining for *HIF-1α* 8 weeks post-

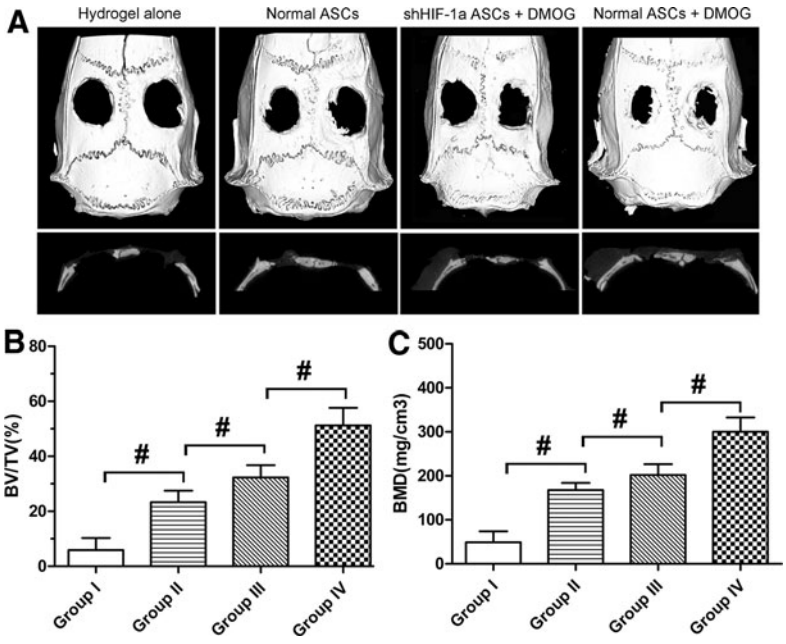

FIG. 5. Micro-CT evaluation of the repaired bone defect at 8 weeks after implantation. **(A)** Micro-CT images of calvarial defects taken 8 weeks after implantation. **(B, C)** Morphometric analysis showed that the bone volume/total volume (BV/TV) and local bone mineral density (BMD) of the newly formed bone in defects varied in each group (#, significant difference between the two groups, $P < 0.05$).

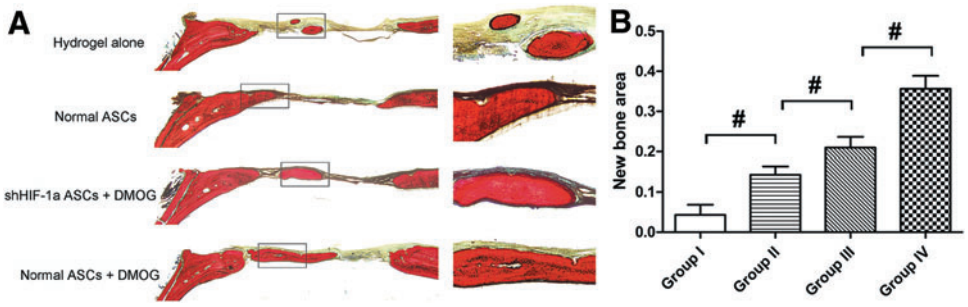

FIG. 6. Histological analysis of newly formed bone in the defect area. **(A)** Representative histological photomicrograph of the newly formed bone in the defect area, which was stained with van Gieson's picrofuchsin. **(B)** Histomorphometric analysis showed that there were significant differences in the new bone area in the different groups (#, significant difference between the two groups, $P < 0.05$). Color images available online at www.liebertpub.com/scd

surgery (Fig. 8A–C). However, positive brown staining was apparent in the bone defect area of Group IV (Fig. 8D). The expression of *OCN*, a late osteogenic marker, in the defect area was also analyzed using immunohistochemistry. The results showed that nearly no positive staining for *OCN* could be found in Group I, a few of positive staining observed in Groups II and III, and more positive staining in Group IV (Fig. 8E–H). Immunohistochemistry for CD31 was performed to evaluate new blood vessel formation in the defect area. Blood vessels were defined with the positive CD31 stain and their typical round or oval structure. The results showed that there were more new vessel formation in Group IV than in other three groups (Fig. 8I–L), which agreed with the micro-CT data.

Discussion

DMOG is a cell-permeable prolyl-4-hydroxylase inhibitor, which can upregulate the protein level of *HIF-1α* post-transcriptionally under normoxic conditions. *HIF-1α* belongs to the Per/Anrt/Sim subfamily of basic helix-loop-helix transcription factors, and plays an important role in bone development and regeneration [30,31]. It also regulates the expression of numerous genes and modulates stem cell proliferation, differentiation, and pluripotency [11]. In this study, we determined whether DMOG improved the osteogenic healing capability of ASCs by activating the expression of *HIF-1α*, and whether DMOG-treated ASCs would be more suitable as seed cells for bone repair and regeneration in tissue engineering.

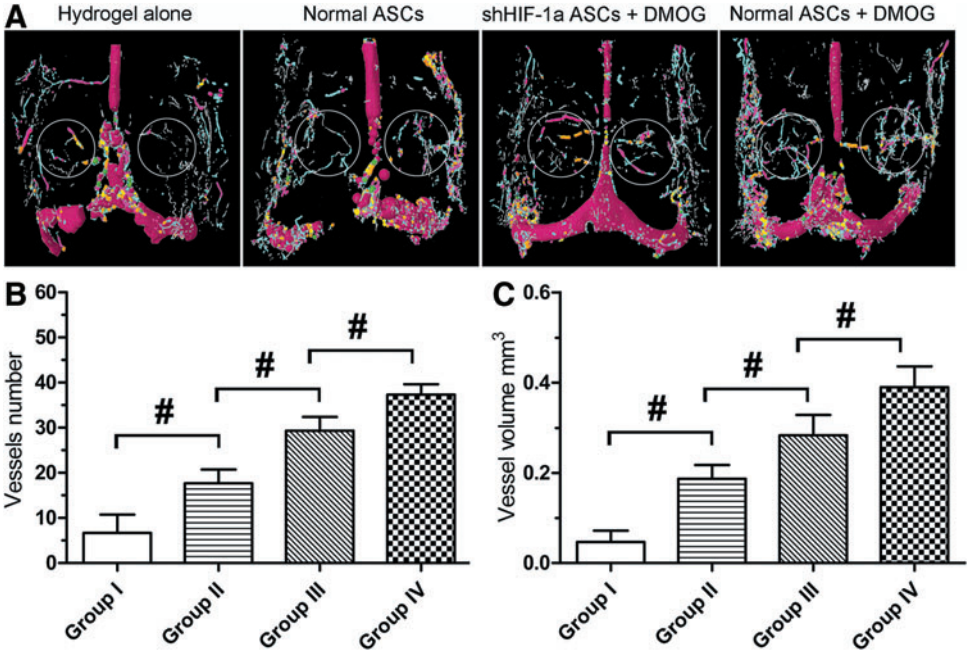

FIG. 7. Micro-CT evaluation of revascularization in the defect area at 8 weeks after implantation. **(A)** Representative images of micro-CT reconstructed three-dimensional microangiography of calvarial defects, which were evaluated from the region of interest (ROI) within the *white frame*. Vessels with various diameters were marked with different colors (*red*: 686–999 μm, *green*: 540–686 μm, *yellow*: 396–504 μm, *orange*: 252–360 μm, *pink*: 144–216 μm, *blue*: 36–108 μm, and *gray*: 1–36 μm). **(B, C)** Quantitative analysis of micro-CT showed mean number of blood vessels and vessel volume in each group (#, significant difference between the two groups, $P < 0.05$). Color images available online at www.liebertpub.com/scd

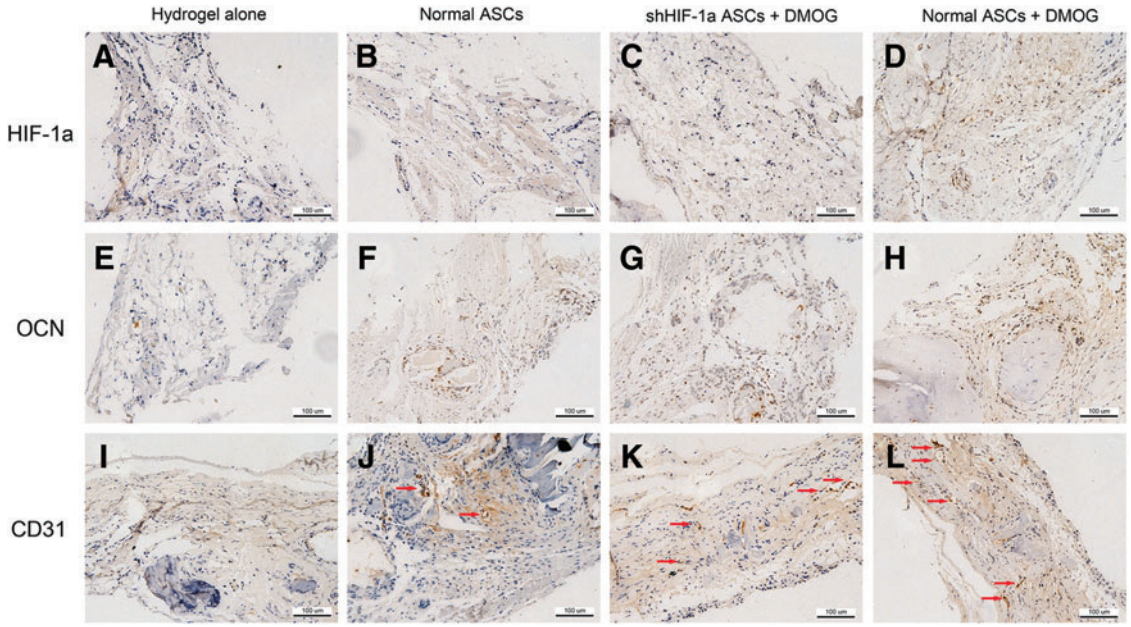

FIG. 8. Immunohistochemical analysis of *HIF-1α*, *OCN*, and CD31 in the defect area of each group at 8 weeks after implantation. There were no obvious positive staining for *HIF-1α* in Groups I **(A)**, II **(B)**, and III **(C)**. However, positive *brown* staining for *HIF-1α* was apparent in Group IV **(D)**. There were nearly no positive staining for *OCN* found in Group I **(E)**, a few of positive staining for *OCN* observed in Groups II **(F)** and III **(G)**, and more positive staining for *OCN* in Group IV **(H)**. Blood vessels were defined with the positive CD31 stain and their typical round or oval structure. Immunohistochemistry for CD31 showed that there were more new vessel formation (*red arrows*) in Group IV **(L)** than in other three groups **(I–K)**. Color images available online at www.liebertpub.com/scd

Using CCK-8, we found that DMOG slightly inhibited ASCs proliferation. However, trypan blue staining showed that DMOG did not cause the death of ASCs at the tested concentrations (up to 1,000 μM), which indicated that DMOG had no obvious cytotoxic effects on ASCs. Previous studies have shown that *HIF-1α* upregulation in cancer cells and neurons participates in cell survival and regulation of cell apoptosis under hypoxic conditions or trophic factor deprivation [32–34]. In this study, we demonstrated that DMOG also inhibited ASCs death induced by serum deprivation in a dose-dependent manner. It was reported that about 90% of transplanted MSCs died on the first day, and no more than 1% survived 4 days after transplantation [35,36]. Therefore, DMOG treatment may enhance ASCs viability in the bone defect area after transplantation, and thereby improve the bone healing capacity of ASCs.

Angiogenic activity of MSCs is regulated by the activation of various signaling pathways, one of which is the *HIF-1* pathway. Under hypoxic conditions, *HIF-1α* is stabilized and accumulated, and subsequently binds to *HIF-1β*. The *HIF-1* complex then activates the expression of *VEGF*. In the present study, western blotting demonstrated that the expression levels of *VEGF* in ASCs were also upregulated when cells were exposed to DMOG, and the increase was dose dependent. However, this increase was significantly inhibited in shHIF-1α ASCs, which indicated that DMOG enhanced the expression of *VEGF* by activating *HIF-1α*.

Using ELISA to detect *VEGF*, we found that the sustained supplement of DMOG led to an obvious increase in the secretion of *VEGF* in ASCs for at least 28 days in vitro. The slow and continued release of *VEGF* is thought to be crucial for angiogenesis in new bone [37,38]. The micro-CT data and immunohistochemistry for CD31 showed that there were more new vessel formation in the group treated with ASCs exposed to DMOG, which supports this point of view. It has been reported that the expression of other angiogenic factors, such as *bFGF*, *Ang-1*, *SDF-1*, *PLGF*, and *SCF*, could also be enhanced by HIF-1α [39–41]. These factors might also be upregulated by DMOG, and aid *VEGF* in the promotion of new vessel formation in the defect areas. The effect of DMOG on these factors will be explored in a future study.

Previous studies found that *HIF-1α* overexpression could directly enhance the osteogenic differentiation potential of MSCs [20,21]. In this study, the results of qRT-PCR, *ALP* activity, and ARS staining demonstrated that DMOG could improve the osteogenic differentiation potential of ASCs in vitro by activating the expression of *HIF-1α*. DMOG-treated ASCs were implanted into critical-sized calvarial defects in rats to explore their capability of promoting bone healing in vivo. Micro-CT and histological examination showed that DMOG could obviously improve the osteogenic healing capability of ASCs in vivo. Immunohistochemistry showed that there were few of positive staining for *HIF-1α* in the bone defect area of group treated with ASCs exposed to DMOG, while nearly no positive staining in other three groups. This demonstrated that DMOG could also activate the expression of *HIF-1α* in vivo. More positive staining for *OCN* was observed in group treated with ASCs exposed to DMOG than other groups, which may be due to that DMOG promotes the osteogenic differentiation of implanted ASCs in vivo.

In this study, bone regeneration in group treated with DMOG-treated shHIF-1α ASCs was more than that in group treated with normal ASCs. This may be because the DMOG contained in hydrogels in Group III affected autologous

BMSCs and ECs, which had not been interfered by *HIF-1α* shRNA and could migrate to the defect area to participate in the repair of bone defects. A previous study demonstrated that the delivery of DMOG from scaffold biomaterials improved angiogenic activity and osteogenic differentiation of nearby BMSCs in vitro [42].

We used hydrogels as cell carriers to evaluate the bone healing capacity of DMOG-treated ASCs. The hydrogel can self-assemble into a 3D nanofiber scaffold, which mimics the extracellular environment and supports cell migration, proliferation, and differentiation within it [43]. Their pore size and porosity are favorable for the transfer of growth factors and invasion of new microvasculars [44]. In addition, DMOG can be loaded in the hydrogels conveniently with sustained release kinetics. However, hydrogels have inherent disadvantages as bone repair materials due to their inadequate osteoconductivity. This study showed that peptide nanofiber hydrogels loaded with DMOG-treated ASCs were not enough to repair the bone defects completely. Many bone substitutes can provide more intrinsic stability and are more beneficial for bone regeneration than hydrogels. These scaffolds loaded with DMOG-treated ASCs may be more suitable in tissue engineering for repairing large bone defects and will be investigated in the future. The application of scaffolds loaded with DMOG, which can release DMOG in a sustained and controlled way in vivo, also deserves to be explored in bone tissue repair.

Conclusion

In summary, our results indicated that DMOG significantly enhanced *VEGF* production in ASCs and improved the osteogenic differentiation potential of ASCs in vitro by stabilizing the expression of *HIF-1α* in ASCs. DMOG-treated ASCs exhibited an increased bone healing capacity in critical defects in vivo, and promoted local revascularization. This study may serve as evidence for further study of the application of DMOG in cell tissue engineering to promote bone healing.

Acknowledgment

This work was supported by the National Natural Science Foundation of China (81101368 and 81272003).

Author Disclosure Statement

No competing financial interests exist.

References

1. Louisia S, M Stromboni, A Meunier, L Sedel and H Petite. (1999). Coral grafting supplemented with bone marrow. J Bone Joint Surg Br 81:719–724.
2. Jo S, S Kim, TH Cho, E Shin, SJ Hwang and I Noh. (2013). Effects of recombinant human bone morphogenic protein-2 and human bone marrow-derived stromal cells on in vivo bone regeneration of chitosan-poly(ethylene oxide) hydrogel. J Biomed Mater Res A 101:892–901.
3. Mariner PD, JM Wudel, DE Miller, EE Genova, SO Streubel and KS Anseth. (2013). Synthetic hydrogel scaffold is an effective vehicle for delivery of INFUSE (rhBMP2) to critical-sized calvaria bone defects in rats. J Orthop Res 31:401–406.
4. Yuan J, L Cui, WJ Zhang, W Liu and Y Cao. (2007). Repair of canine mandibular bone defects with bone marrow stromal cells and porous beta-tricalcium phosphate. Biomaterials 28:1005–1013.
5. Liu G, L Zhao, W Zhang, L Cui, W Liu and Y Cao. (2008). Repair of goat tibial defects with bone marrow stromal cells and beta-tricalcium phosphate. J Mater Sci Mater Med 19:2367–2376.
6. Cowan CM, YY Shi, OO Aalami, YF Chou, C Mari, R Thomas, N Quarto, CH Contag, B Wu and MT Longaker. (2004). Adipose-derived adult stromal cells heal critical-size mouse calvarial defects. Nat Biotechnol 22:560–567.
7. Dudas JR, KG Marra, GM Cooper, VM Penascino, MP Mooney, S Jiang, JP Rubin and JE Losee. (2006). The osteogenic potential of adipose-derived stem cells for the repair of rabbit calvarial defects. Ann Plast Surg 56:543–548.
8. Geiger F, H Bertram, I Berger, H Lorenz, O Wall, C Eckhardt, HG Simank and W Richter. (2005). Vascular endothelial growth factor gene-activated matrix (VEGF165-GAM) enhances osteogenesis and angiogenesis in large segmental bone defects. J Bone Miner Res 20:2028–2035.
9. Hiltunen MO, M Ruuskanen, J Huuskonen, AJ Mahonen, M Ahonen, J Rutanen, VM Kosma, A Mahonen, H Kroger and S Yla-Herttuala. (2003). Adenovirus-mediated VEGF-A gene transfer induces bone formation in vivo. FASEB J 17:1147–1149.
10. Riddle RC, R Khatri, E Schipani and TL Clemens. (2009). Role of hypoxia-inducible factor-1alpha in angiogenic-osteogenic coupling. J Mol Med (Berl) 87:583–590.
11. Mazumdar J, V Dondeti and MC Simon. (2009). Hypoxia-inducible factors in stem cells and cancer. J Cell Mol Med 13:4319–4328.
12. Ferrara N. (1999). Molecular and biological properties of vascular endothelial growth factor. J Mol Med (Berl) 77: 527–543.
13. Gerber HP and N Ferrara. (2000). Angiogenesis and bone growth. Trends Cardiovasc Med 10:223–228.
14. Winet H. (1996). The role of microvasculature in normal and perturbed bone healing as revealed by intravital microscopy. Bone 19:39S–57S.
15. Glowacki J. (1998). Angiogenesis in fracture repair. Clin Orthop Relat Res 355 Suppl:S82–S89.
16. Street J and B Lenehan. (2009). Vascular endothelial growth factor regulates osteoblast survival—evidence for an autocrine feedback mechanism. J Orthop Surg Res 4:19.
17. Clarkin CE, RJ Emery, AA Pitsillides and CP Wheeler-Jones. (2008). Evaluation of VEGF-mediated signaling in primary human cells reveals a paracrine action for VEGF in osteoblast-mediated crosstalk to endothelial cells. J Cell Physiol 214:537–544.
18. Midy V and J Plouet. (1994). Vasculotropin/vascular endothelial growth factor induces differentiation in cultured osteoblasts. Biochem Biophys Res Commun 199:380–386.
19. Nagano M, K Kimura, T Yamashita, K Ohneda, D Nozawa, H Hamada, H Yoshikawa, N Ochiai and O Ohneda. (2010). Hypoxia responsive mesenchymal stem cells derived from human umbilical cord blood are effective for bone repair. Stem Cells Dev 19:1195–1210.
20. Ding H, YS Gao, C Hu, Y Wang, CG Wang, JM Yin, Y Sun and CQ Zhang. (2013). HIF-1alpha transgenic bone marrow cells can promote tissue repair in cases of corticosteroid-induced osteonecrosis of the femoral head in rabbits. PLoS One 8:e63628.

21. Zou D, Z Zhang, J He, S Zhu, S Wang, W Zhang, J Zhou, Y Xu, Y Huang, et al. (2011). Repairing critical-sized calvarial defects with BMSCs modified by a constitutively active form of hypoxia-inducible factor-1alpha and a phosphate cement scaffold. Biomaterials 32:9707–9718.
22. Zou D, Z Zhang, D Ye, A Tang, L Deng, W Han, J Zhao, S Wang, W Zhang, et al. (2011). Repair of critical-sized rat calvarial defects using genetically engineered bone marrow-derived mesenchymal stem cells overexpressing hypoxia-inducible factor-1alpha. Stem Cells 29:1380–1390.
23. Jaakkola P, DR Mole, YM Tian, MI Wilson, J Gielbert, SJ Gaskell, A von Kriegsheim, HF Hebestreit, M Mukherji, et al. (2001). Targeting of HIF-alpha to the von Hippel-Lindau ubiquitylation complex by O2-regulated prolyl hydroxylation. Science 292:468–472.
24. Ockaili R, R Natarajan, F Salloum, BJ Fisher, D Jones, AA Fowler 3rd and RC Kukreja. (2005). HIF-1 activation attenuates postischemic myocardial injury: role for heme oxygenase-1 in modulating microvascular chemokine generation. Am J Physiol Heart Circ Physiol 289:H542–H548.
25. Song YR, SJ You, YM Lee, HJ Chin, DW Chae, YK Oh, KW Joo, JS Han and KY Na. (2010). Activation of hypoxia-inducible factor attenuates renal injury in rat remnant kidney. Nephrol Dial Transplant 25:77–85.
26. Milkiewicz M, CW Pugh and S Egginton. (2004). Inhibition of endogenous HIF inactivation induces angiogenesis in ischaemic skeletal muscles of mice. J Physiol 560:21–26.
27. Nagel S, M Papadakis, R Chen, LC Hoyte, KJ Brooks, D Gallichan, NR Sibson, C Pugh and AM Buchan. (2011). Neuroprotection by dimethyloxalylglycine following permanent and transient focal cerebral ischemia in rats. J Cereb Blood Flow Metab 31:132–143.
28. Estes BT, BO Diekman, JM Gimble and F Guilak. (2010). Isolation of adipose-derived stem cells and their induction to a chondrogenic phenotype. Nat Protoc 5:1294–1311.
29. Rohrer MD and CC Schubert. (1992). The cutting-grinding technique for histologic preparation of undecalcified bone and bone-anchored implants. Improvements in instrumentation and procedures. Oral Surg Oral Med Oral Pathol 74: 73–78.
30. Wan C, J Shao, SR Gilbert, RC Riddle, F Long, RS Johnson, E Schipani and TL Clemens. (2010). Role of HIF-1alpha in skeletal development. Ann N Y Acad Sci 1192:322–326.
31. Shomento SH, C Wan, X Cao, MC Faugere, ML Bouxsein, TL Clemens and RC Riddle. (2010). Hypoxia-inducible factors 1alpha and 2alpha exert both distinct and overlapping functions in long bone development. J Cell Biochem 109:196–204.
32. Lomb DJ, JA Straub and RS Freeman. (2007). Prolyl hydroxylase inhibitors delay neuronal cell death caused by trophic factor deprivation. J Neurochem 103:1897–1906.
33. Sasabe E, Y Tatemoto, D Li, T Yamamoto and T Osaki. (2005). Mechanism of HIF-1alpha-dependent suppression of hypoxia-induced apoptosis in squamous cell carcinoma cells. Cancer Sci 96:394–402.
34. Piret JP, C Lecocq, S Toffoli, N Ninane, M Raes and C Michiels. (2004). Hypoxia and CoCl2 protect HepG2 cells against serum deprivation- and t-BHP-induced apoptosis: a possible anti-apoptotic role for HIF-1. Exp Cell Res 295:340–349.
35. Tang YL, Y Tang, YC Zhang, K Qian, L Shen and MI Phillips. (2005). Improved graft mesenchymal stem cell survival in ischemic heart with a hypoxia-regulated heme oxygenase-1 vector. J Am Coll Cardiol 46:1339–1350.
36. Toma C, MF Pittenger, KS Cahill, BJ Byrne and PD Kessler. (2002). Human mesenchymal stem cells differentiate to a cardiomyocyte phenotype in the adult murine heart. Circulation 105:93–98.
37. Nikol S, MG Engelmann, J Pelisek, A Fuchs, A Golda, M Shimizu, C Mekkaoui and PH Rolland. (2002). Local perivascular application of low amounts of a plasmid encoding for vascular endothelial growth factor (VEGF165) is efficient for therapeutic angiogenesis in pigs. Acta Physiol Scand 176:151–159.
38. Elcin YM, V Dixit and G Gitnick. (2001). Extensive in vivo angiogenesis following controlled release of human vascular endothelial cell growth factor: implications for tissue engineering and wound healing. Artif Organs 25:558–565.
39. Forsythe JA, BH Jiang, NV Iyer, F Agani, SW Leung, RD Koos and GL Semenza. (1996). Activation of vascular endothelial growth factor gene transcription by hypoxia-inducible factor 1. Mol Cell Biol 16:4604–4613.
40. Ceradini DJ, AR Kulkarni, MJ Callaghan, OM Tepper, N Bastidas, ME Kleinman, JM Capla, RD Galiano, JP Levine and GC Gurtner. (2004). Progenitor cell trafficking is regulated by hypoxic gradients through HIF-1 induction of SDF-1. Nat Med 10:858–864.
41. Kelly BD, SF Hackett, K Hirota, Y Oshima, Z Cai, S Berg-Dixon, A Rowan, Z Yan, PA Campochiaro and GL Semenza. (2003). Cell type-specific regulation of angiogenic growth factor gene expression and induction of angiogenesis in nonischemic tissue by a constitutively active form of hypoxia-inducible factor 1. Circ Res 93:1074–1081.
42. Wu C, Y Zhou, J Chang and Y Xiao. (2013). Delivery of dimethyloxallyl glycine in mesoporous bioactive glass scaffolds to improve angiogenesis and osteogenesis of human bone marrow stromal cells. Acta Biomater 9:9159–9168.
43. Amini AA and LS Nair. (2012). Injectable hydrogels for bone and cartilage repair. Biomed Mater 7:024105.
44. Hosseinkhani H, M Hosseinkhani, A Khademhosseini, H Kobayashi and Y Tabata. (2006). Enhanced angiogenesis through controlled release of basic fibroblast growth factor from peptide amphiphile for tissue regeneration. Biomaterials 27:5836–5844.

Address correspondence to:
Dr. Changqing Zhang
Department of Orthopedic Surgery
Shanghai Sixth People's Hospital
Shanghai Jiao Tong University
600 Yishan Road
Shanghai 200233
China

E-mail: zcqgk@hotmail.com

Dr. Yuan Sun
Department of Orthopedic Surgery
Shanghai Sixth People's Hospital
Shanghai Jiao Tong University
600 Yishan Road
Shanghai 200233
China

E-mail: david1979982@163.com

Received for publication October 8, 2013
Accepted after revision December 13, 2013
Prepublished on Liebert Instant Online December 13, 2013